

# Task–Effector Asymmetries in a Rhythmic Continuation Task

Hong Yu  
Pennsylvania State University

Daniel M. Russell  
Berks–Lehigh Valley College, Pennsylvania State University

Dagmar Sternad  
Pennsylvania State University

Variability in rhythmic movements has been interpreted as a signature of internal or peripheral noise processes. Grounded in an oscillator interpretation, this study hypothesized that period variability and drift arises from the asymmetry between target period and the limb's intrinsic dynamics. Participants synchronized to 7 target periods, swinging 1 of 3 pendulums in a continuation paradigm; 3 periods were longer, 3 shorter, and 1 identical to the preferred period. Results supported 5 predictions: Drift toward the preferred period was observed that scaled with the asymmetry. Variability was lowest for symmetry conditions and increased with the asymmetry. Variability decreased concomitant with the approach toward the preferred period. Periods exponentially approached the preferred period with positive autocorrelations up to 10 cycles.

If limb segments of the human body swing rhythmically in the gravitational field, such as legs and arms move rhythmically in walking, it has been a straightforward first step to capture their spatiotemporal behavior as pendular movements. From classical mechanics it follows that these limb segments, conceived as self-sustained pendular movements, have a tendency to oscillate at their characteristic frequency, or eigenfrequency, which is determined by the segment's length and mass distribution. That this eigenfrequency plays an important role in movement coordination has for instance been argued in studies on locomotion where preferred walking or running speeds were associated with least energy consumption. Conversely, minimum energy consumption has been interpreted as indicative of animals utilizing the mechanically and energetically optimal coordination mode (Holt, Jeng, Ratcliffe, & Hamill, 1995; Hoyt & Taylor, 1981; Sparrow & Newell, 1994; Turvey, Schmidt, Rosenblum, & Kugler, 1988).

For acting successfully within the demands and constraints of the environment, however, it is similarly important for the organism not only to exploit such mechanical properties but also to override them when the task requires it. For example, humans can easily walk faster or slower depending on their goal. They also have little difficulty in synchronizing finger taps or foot steps in

dancing to a wide range of rhythms. This observation has found support in experimental research that showed that tapping to specific metronome periods can be equally achieved with finger, wrist, and elbow movements (Collyer, Broadbent, & Church, 1992; Wing, 1977). Similarly, rhythmically moving visual targets can be tracked using manipulanda of varying mechanical properties for a wide range of frequencies (Noble, Fitts, & Warren, 1955; Pew, Duffendack, & Fensch, 1967; Russell & Sternad, 2001).

Despite this ability to override intrinsic tendencies and to adapt to external timing demands, there is evidently a cost as well as limits to this range that are likely to be determined by the difference between the eigenfrequency of the particular effector and the target frequency. It has been demonstrated experimentally that it is difficult to move a limb or a manipulandum at a frequency much faster than its respective eigenfrequency (Noble et al., 1955; Poulton, 1974). Similarly, it can be arduous to slow down an effector to a frequency much slower than its eigenfrequency. This difference between the effector eigenfrequency and the target frequency is referred to as the task–effector asymmetry and is of central interest in this study. In previous research, we have addressed this issue in visuomotor tracking of sinusoidally moving targets with continuous feedback by explicit quantitative manipulations of both target and eigenfrequency (Russell & Sternad, 2001). We demonstrated that tracking behavior, specifically its variability, was a function of this asymmetry, rather than simply a function of the absolute target frequency. Relatedly, Russell, de Rugy, and Sternad (2003) reported systematic phase leads and lags as a function of this asymmetry in tracking visual stimuli both with and without visual feedback. These results were consistent with results found in bimanual rhythmic coordination (e.g., Sternad, Amazeen, & Turvey, 1996).

What remains an open issue, however, is how such asymmetry between the effector and the task influences the behavior, once the perceptual target is no longer available. Specifically, experiments

---

Hong Yu and Dagmar Sternad, Department of Kinesiology, Pennsylvania State University; Daniel M. Russell, Division of Science, Berks–Lehigh Valley College, Pennsylvania State University.

This research was supported by National Science Foundation Research Grant SBR 97-10312 and Behavioral Neuroscience Grant 00-96543 awarded to Dagmar Sternad. We thank Tjeerd Dijkstra for many helpful discussions.

Correspondence concerning this article should be addressed to Dagmar Sternad, Department of Kinesiology, Pennsylvania State University, 266 Recreation Building, University Park, Pennsylvania 16802. E-mail: dxs48@psu.edu

on rhythmic timing have frequently used the so-called *continuation paradigm*, where participants continue rhythmic movements after an external pacemaker has been turned off. How the rhythm is maintained without the guidance of an external clock has been the focus of many studies with the objective of revealing timing mechanisms in humans. The present study investigates such continued rhythmic movements at different target frequencies with the objective of assessing the role of task–effector asymmetries in such rhythmic performance.

Early work on the timing of oscillatory movements was performed by von Holst (1939/1973) using spinal fish preparations as his primary model system. If each fin is considered to be an oscillator with a resonance frequency, two or more fins (or limbs) when moving together at the same frequency and fixed phase difference are said to move in absolute coordination. In absolute coordination, von Holst formulated two processes that are in conflict with each other: The magnet effect conceptualizes the tendency of two rhythms to synchronize at one common frequency and a fixed phase relation. The maintenance tendency captures the propensity for each oscillator to move at its own characteristic frequency. If the maintenance tendency prevails, the oscillators will move at their preferred frequencies and their phase relation will start to wander (relative coordination). It is the competition and cooperation expressed in these two tendencies that gives rise to the observed behavior. Of particular interest for the present study is one of von Holst's observations on the synchronization between pectoral and dorsal fin, each having its own eigenfrequency. Although the pectoral and dorsal fins of a transected labrus fish easily synchronize to oscillate at the same frequency, the dorsal fin immediately reestablishes its own rhythm once the pectoral fin is inhibited (see also Figure 4.21 in Turvey & Carello, 1995; von Holst, 1939/1973). It is this finding that has motivated the present experiment. The hypothesis we test in this study is that rhythmic movements that were initially guided by an external target rhythm have an inclination to drift toward their eigenfrequency once the external timekeeper is turned off.

Inspired by von Holst (1939/1973), absolute coordination has been investigated in humans, using a bimanual rhythmic coordination task in which participants oscillate a pendulum held in each hand at one common frequency, either in a parallel (inphase) or alternating (antiphase) fashion (Kugler & Turvey, 1987). The advantage of this experimental task is that the eigenfrequencies of the wrist–pendulum system can be manipulated and calculated using standard mechanical algorithms. Asymmetries were introduced by having participants swing pendulums of different eigenfrequencies in each hand. Achieving absolute coordination under widely different pendulum combinations, actors settled on a combined movement frequency that was in between the eigenfrequency of each pendulum, corresponding to the frequency determined for rigidly coupled pendulums following Huygens's law (Kugler & Turvey, 1987). In a series of studies the coupled oscillator model was further analyzed and predictions about steady state relative phase and its fluctuations were derived and experimentally confirmed: first, the larger the asymmetry, the greater the phase difference between the two oscillations. The oscillator with the faster intrinsic frequency tends to lead. Second, the degree of fluctuations in continuous relative phase increases with increasing asymmetry between the two wrist pendulums. The larger the difference in the two oscillators' intrinsic frequencies, the less

stable is the pattern, that is, more prone to fluctuations (Collins, Sternad, & Turvey, 1996; Schmidt, Shaw, & Turvey, 1993; Sternad et al., 1996; Sternad, Collins, & Turvey, 1995; Sternad, Turvey, & Schmidt, 1992). These phenomena are a major motivation for the present study.

The control of rhythm and timing has been the focus of an extensive body of literature that has pursued different theoretical concepts. Although the above-referenced studies pursued the concept of coupled oscillations, more cognitive theories paid particular attention to the notion of an intrinsic clock or timekeeping mechanism underlying the production of rhythmic intervals (e.g., Bartlett & Bartlett, 1959; Collyer & Church, 1998; Ivry & Hazeltine, 1995; Ivry & Richardson, 2002; Stevens, 1886; Wing & Kristofferson, 1973a, 1973b). In order to reveal the nature of this clocking mechanism, these studies have frequently used the continuation paradigm where this hypothesized endogenous timing can be discerned most clearly. Results of these studies agree that, although humans are relatively accurate in maintaining the correct tapping period even after the metronome has been removed, systematic deviations and drifts occur when a range of target periods is investigated. One of the early continuation finger-tapping studies by Stevens reported that subjects most accurately reproduced the target period close to 0.71 s, which he referred to as the indifference point. Although no explanation was given, it may be conjectured that this indifference point corresponded to the eigenfrequency of the effector.

Similarly, drifts in the movement period have been observed across the continuation interval, especially when the continuation interval is longer. Sternad, Dean, and Newell (2000) reported a consistent shortening of the tapping period across a 50-s interval. Madison (2001) reported period drifts that vary systematically with the intertap interval and that show discontinuous changes at critical periods. In contrast, Collyer and colleagues observed period errors that showed a W-shaped pattern when plotting the produced period as a percentage of the target period across different target periods (0.175–1.00 s; Collyer, Boatright-Horowitz, & Hooper, 1997; Collyer et al., 1992; Collyer, Broadbent, & Church, 1994; Collyer & Church, 1998). The authors attributed their findings to discrete internal clock mechanisms where an ensemble of clocks produces discrete rhythms that are attractive for rhythms adjacent to them (Church & Broadbent, 1991). The alternative interpretation that biomechanical factors are responsible for the small systematic deviations was rejected, as wrist and finger movements produced a congruent “oscillator signature” (Collyer et al., 1994).

This conclusion contrasts with other studies that have shown the central role of the mechanically and muscularly determined resonance frequency as an anchor point for rhythmic movements (Goodman, Riley, Mitra, & Turvey, 2000; Hatsopoulos, 1996; Hatsopoulos & Warren, 1996). In order to clarify the role of resonance frequency and task–effector asymmetry in a continuation task, the present study undertakes a systematic empirical manipulation of the mechanical properties of the effector in relation to the target frequency. The hypothesis is that it is the discrepancy between the frequency of the target and the eigenfrequency of the moving limb that is responsible for period deviations and variability in the continuation interval. This discrepancy is systematically manipulated and quantified in the independent vari-

able  $\delta$  that is defined as the difference between target period and resonance period (for more details see the Method section).

The experiment consists of seven target periods, calculated to be symmetric around the eigenperiod or preferred period. Participants track each of the visually presented target periods with one of three handheld pendulums, each of a different eigenperiod. The synchronization segment  $S$  (20 s) is followed by a deliberately long continuation segment of 60 s in order to allow for drifts to develop. The 60-s long continuation segment  $C$  is divided into three equally long segments,  $C1$ ,  $C2$ , and  $C3$ . The focus of the analyses is on changes in the mean period and amplitudes and their variability across the continuation segments. On the basis of the preceding arguments and findings, we can formulate five predictions that are illustrated schematically in Figure 1 (for more detail see the Appendix). During the continuation interval rhythmic movements drift toward their resonance period. Figure 1A sketches this prediction by showing the period drift or deviation against the asymmetry between the target and eigenperiod of the limb captured in  $\delta$ .

1. There is a positive drift (acceleration) for eigenperiods faster than the target and a negative drift (deceleration) for eigenperiods slower than the target.

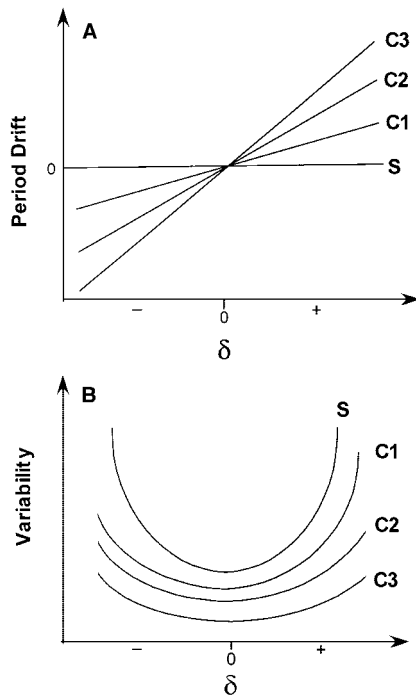


*Figure 1.* Schematic predictions for period drift as a function of task-effector asymmetry  $\delta$ . A: Drifts increase with increasing asymmetry between the two oscillations. During the synchronization segment  $S$ , no period deviations are expected. The drifts should increase during the continuation segments from  $C1$  through  $C3$ . B: Variability is predicted to be lowest for task-effector symmetry ( $\delta = 0$ ). With increasing task-effector asymmetry ( $\delta \neq 0$ ), variability is expected to increase in a symmetric fashion. Large differences between target and preferred period in  $S$  are expected to be accompanied by highest variability. With increasing period drift in  $C$ , variability should decrease accordingly.

2. The larger the asymmetry between target period and eigenperiod, the larger the drift.
3. Variability of movement periods is at a minimum when there is symmetry between target and eigenperiod ( $\delta = 0$ ). It increases in a U-shaped fashion with increasing  $\delta$  (see Figure 1B).
4. Variability is highest during the synchronization segment  $S$  as the asymmetry between target period and the preferred period has to be maintained. Accompanying the drift toward the resonance period, variability decreases throughout the continuation segments  $C1$ ,  $C2$ ,  $C3$  (Figure 1B).
5. The drift in period toward the resonance period progresses exponentially.

## Method

### Participants

Six participants (4 male and 2 female) from Pennsylvania State University participated as volunteers in this experiment. Their ages ranged from 23 to 42 years. All reported themselves right-handed with normal or corrected-to-normal eyesight. Of the participants, 4 had participated in a similar previous experiment; the remaining 2 were new to the task. They all agreed to the experimental procedures by signing the informed consent form required by the University Regulatory Committee.

### Apparatus and Materials

Participants sat in a specially built chair and placed their forearms on the horizontal armrests provided. They grasped a pendulum in their dominant hand and swung it in the sagittal plane (see Figure 2). In order to record the pendulum's movement trajectory in 3-D, a Sonic Digitizer (SAC Corporation, Stratford, CT) was used, which recorded sound sparks made by an emitter attached to the tip of the pendulum at a rate of 60 Hz. The sound was detected by four microphones arranged in a square on the floor ( $77 \times 77$  cm). As only three recordings were necessary to locate the emission point in 3-D, the worst of the four readings was automatically eliminated from the analysis. The chair had an elevated leg rest and was attached to one side of an enclosure so that the legs did not obscure the sound from the emitter on the pendulum to the four microphones. The sides and the floor of the enclosure were covered with sound-proofing egg-crate foam to reduce reflection errors. Armrests were provided to localize the axis of rotation of the combined wrist-pendulum system and to ensure that the participants only swung the pendulums using radial and ulnar flexion around the axis of rotation in the wrist joint.

Participants swung one pendulum in their dominant hand. Three pendulums of different eigenperiods were assembled: (a) a 36-cm long pendulum, giving an eigenperiod of 800 ms; (b) a 40-cm long pendulum with 50-g weight attached, giving an eigenperiod of 1,000 ms; and (c) a 48-cm long pendulum with 150-g weight attached, giving an eigenperiod of 1,200 ms. (Note that we use periods instead of frequencies to be in better agreement with the conventions in the literature on timing.) The calculations of the pendulums' eigenperiods or eigenfrequencies  $\omega$  of the wrist-pendulum systems applied the standard formula

$$\omega = 2\pi \left( \frac{g}{L} \right)^{1/2} \text{ (rad/s)},$$

where  $g$  is the constant acceleration due to gravity.  $L$  is the equivalent length of the wrist-pendulum, defined as the distance between the center of

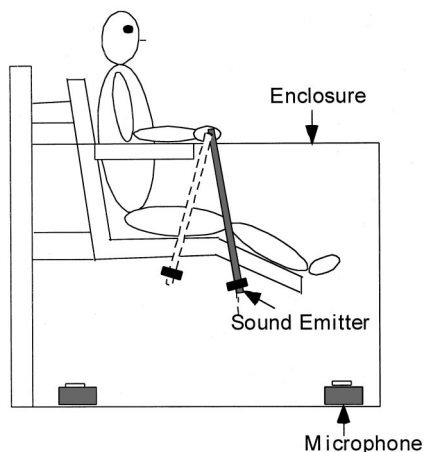


Figure 2. Experimental apparatus.

rotation and the center of mass. The center of mass was calculated from the pendulum components shaft length, added mass, and hand mass through the standard methods for representing an arbitrary rigid body oscillating around a fixed point of rotation as a simple pendulum. The axis of rotation was centered in the wrist. All components including the hand were modeled as hollow cylinders. The hand mass was approximated as 0.6% of an average body mass of 75 kg (Bernstein, 1967; Dempster, 1955). More details of the computations are described in Kugler and Turvey (1987). On the basis of the calculated center of mass and equivalent length of the compound system  $L$  oscillating around the axis of rotation at the wrist,  $\omega$  and its eigenperiod was determined. The wrist-pendulums' eigenperiods were chosen to be distinctly different from each other. A limiting factor for the choice of the long and heavy pendulum was potential fatigue for participants; for the small pendulum, sufficient length was necessary to provide good digitizer readings.

From the raw position data in three Cartesian dimensions, the angular displacement of the pendulum's tip around the axis of rotation in the sagittal plane was calculated and stored on a Master Computer 486 DX 266 PCI, using custom-written motion analysis software. The target movement and the pendulum's tracking movement were displayed on an Acerview-7155 monitor (resolution:  $640 \times 480$  pixels) situated in front of the participant (1.50 m from the back of the chair) and approximately in line with the participant's eye level. The monitor screen was 1.20 m from the participant's eyes, although his or her head position was not constrained. The room lights were dimmed to enhance the contrast of the visual display on the screen. Each trial consisted of a synchronization phase and a continuation phase. During the synchronization phase a hollow green target square ( $1 \times 1$  cm), creating a visual angle of  $0.5^\circ$ , moved in a sinusoidal motion in the vertical direction on the monitor. The movements of the pendulum's tip were displayed as a green hair cross ( $1 \times 1$  cm) on the monitor screen that represented the pendulum's angular position in the sagittal plane. The cursor was constrained to move in the same vertical direction on the monitor as the target square, corresponding to pendular movements in the sagittal plane. The peak-to-valley amplitude of the sine wave was kept constant at 0.52 rad for all frequency conditions, creating a vertical movement of 11.6 cm on the screen and traversing a visual angle of  $5^\circ$  (0.1 rad) at the eye. This amplitude was the average preferred amplitude determined in pilot testing.

### Procedure and Design

The experiment consisted of three sessions that were run on the same or on consecutive days. In each session one pendulum was tested. The order

of presentation of the pendulums was randomized across participants. In the first part of each session participants were instructed to swing the pendulum in the sagittal plane with the dominant hand at the period and amplitude they preferred. There was no display shown on the monitor. The objective was to determine the individually preferred period and amplitude for each of the three pendulums. Three trials were collected, each lasting 40 s. The three trials were performed in quick succession, sometimes even without a stop, so that they effectively could be regarded as a single trial of 120 s.<sup>1</sup> Immediately after these trials, the experimenter calculated the average period of each trial and the overall average across the three trials. On the basis of each participant's preferred period, seven target periods were calculated for each pendulum: Three target periods faster than the preferred periods were calculated by subtracting 50 ms, 100 ms, and 150 ms from the preferred period. Three slower periods were calculated by adding 50 ms, 100 ms, and 150 ms to the preferred period. As these target periods differed in absolute values, we introduced the independent variable  $\delta$  that captured this asymmetry. It was defined as

$$\delta = \text{target period} - \text{preferred period}.$$

This definition allowed a comparison across participants who all displayed slightly different preferred periods. Consequently,  $\delta$  was negative between  $-150$  ms and  $-50$  ms for target periods shorter than the preferred period, and positive between 50 ms and 150 ms for target periods longer than the preferred period.  $\delta = 0$  refers to the symmetry condition where the target period was set to match the preferred period.

Immediately after the preparation of the target periods, which lasted approximately 20 min, data were collected. It was deemed important to have the preferred period calculations and the actual experiment immediately following each other, so that conditions of the participant and the intrinsically preferred period would not change. Two trials were run for each of the seven target periods, presented in random order within each of the three sessions. All trials consisted of a synchronization segment and a continuation segment. In the synchronization segment  $S$  (20 s), both the sinusoidally moving target and the online display of the pendulum's movement were shown on the screen. Participants were instructed to track the target by swinging the pendulum in the sagittal plane, trying to keep the cross in the target square on the screen. Immediately after  $S$ , the participants were instructed to close their eyes and maintain their pendulum movements with the same period and amplitude. The entire continuation segment  $C$  lasted 65 s. For the analysis, the first 5 s of  $C$  were discarded to eliminate short-term transients or perturbations due to the closing of the eyes. The remaining 60 s were subdivided into three equal intervals of 20 s duration each, referred to as  $C1$ ,  $C2$ , and  $C3$ . Hence, each trial lasted for a total of 85 s, plus 5-s lead-in time, where only the target was moving on the screen to allow the participant to adjust to the target motion before data collection started.

Throughout the experiment participants were required to maintain their forearms on the armrest and to grasp the pendulum firmly enough so that no movement occurred within the hand. The task was always performed with their dominant right hand. Participants could rest between trials if necessary to avoid fatigue.

### Data Reduction and Dependent Measures

The time series of the pendulum's angular position for each trial was low-pass filtered using a zero-lag second-order Butterworth filter with a

<sup>1</sup> The duration of 40 s for each of the three trials was regarded sufficient to estimate the preferred period. As shown in Table 1, which is presented later in this article, the estimates of the three trials were within a very small range. Inspection of the three trial means of one participant's performance showed that there was no systematic ordering that could indicate a systematic drift. Hence, a drift is not inherent in this long trial at the preferred period.

cutoff frequency at 8 Hz. This filter cutoff frequency was automatically determined using a procedure that varied the cutoff frequency and approximated the difference between the filtered and unfiltered data using the autocorrelation function (Challis, 1999). The cutoff frequency is the one in which the autocorrelation function most closely resembled white noise. The angular velocity was computed using a two time-step differentiation procedure. The first 3 s of each time series were excluded from the analysis, as they were confounded with transient effects when the participant attempted to match the target movements with the pendulum. Each time series was then parsed into four segments: synchronization segment (S) from 1 to 20 s, Continuation Segment 1 (C1) from 25 to 45 s, Continuation Segment 2 (C2) from 45 to 65 s, and Continuation Segment 3 (C3) from 65 to 85 s. Every dependent measure was then computed separately for each of the four segments of each trial. Global cycle measures of the segmented time series of the pendulum angular position were determined, including means and standard deviations of both peak-to-peak period  $T$  and peak-to-valley amplitude  $A$ . For each segment the deviation of the actual period from the target period was calculated as

$$\Delta T = \text{target period} - \text{actual period}.$$

$\Delta T$  was calculated for each cycle period and as a mean for each segment. All dependent measures were computed using software written in Matlab.

### Harmonicity

To capture the variability of the trajectory in comparison to a smooth harmonic wave, a measure called *harmonicity* ( $H$ ) was computed. The dependent measure was determined in phase space, that is, the space spanned by angular position and velocity. The time series was separated into the four segments as described above. Prior to computing  $H$  the position trace was mean adjusted by subtracting the average pendulum position from the time series to center the trajectory around zero. The angular velocity was normalized by dividing the velocity signal by the primary movement frequency. The mean adjusted position and normalized velocity were then used to create the normalized phase portrait, from which the phase angle of the pendulum was determined as the arctangent of the mean adjusted position and normalized velocity (Sternad et al., 1996). The radius for each sample was calculated by using Pythagoras's theorem. After calculating the average radius ( $r$ ) across the whole trajectory of one trial, the time series of  $r$  was divided by this mean to normalize the phase portrait to a radius of one. A harmonic wave is characterized by a perfect unit circle in phase space after normalization of velocity. Subsequently, the radius of the sine wave was subtracted from  $r$  and the remainder was summed similar to a root mean square error. This measure  $H$  captures the difference between the trajectory's limit cycle and a harmonic wave. Large values of  $H$  indicate large departures from a smooth harmonic wave (Sternad, Turvey, & Saltzman, 1999).

### Clock and Motor Variance

On the basis of the assumption of two independent processes representing the central clock and the peripheral levels, each associated with independent Gaussian noise, the analysis developed by Wing and Kristofferson (1973a) quantifies the relative contribution of these two sources of noise to the observed variance. The Wing-Kristofferson model makes two specific predictions with regard to the autocorrelation functions of successive cycle periods. First, the Lag 1 autocorrelation  $\rho(1)$  is between 0 and  $-0.5$ ; second, for lags greater than one the autocorrelation is 0. Hence, both  $\rho(1)$  and Lag 2  $\rho(2)$  autocorrelations of cycle period were determined. Prior to the calculation of the autocorrelation functions, the cycle periods  $T_p$  were linearly detrended, in order to remove systematic drifts in the cycle periods (Vorberg & Wing, 1996). For the segments of trials that met both of the predictions of the Wing-Kristofferson model, the period variance

( $s_T^2$ ) was computed, and then clock ( $s_c^2$ ) and motor ( $s_m^2$ ) variance were calculated using the following equations:

$$\text{cov}(T_{p,j}, T_{p,j-1}) = -s_m^2, \quad (1)$$

and

$$s_T^2 = s_c^2 + 2s_m^2, \quad (2)$$

where  $j$  denotes two abutting cycle periods. For further details, see Wing and Kristofferson (1973a, 1973b) and Vorberg and Wing (1996).

Each dependent variable was analyzed separately using a three-way repeated measures analysis of variance (ANOVA) with the three factors: pendulum (3 levels),  $\delta$  (7 levels), and segment (4 levels). All significant effects are reported; nonsignificant results are omitted. To test the nonlinear behavior predicted for variability estimates as a function of  $\delta$  (Predictions 3 and 4), polynomial regressions were conducted. If this effect was significant, additional ANOVAs tested the differential effect for the different segments.

## Results

### Preferred Periods and Amplitudes

Three pendulums were assembled to determine three different eigenperiods for the moving limb. However, as discussed in previous work, the individual's preferred period is not necessarily identical to the eigenperiod that is calculated on the basis of mechanical components of the pendulum plus a standard estimate of the hand mass. The neuromuscular components constitute an additional important factor that is not captured in the mechanically based calculations of the eigenperiod (Hatsopoulos & Warren, 1996). To obtain a more accurate estimate for the individuals' preferred period, all participants therefore performed preparatory trials in which they swung the handheld pendulums in their preferred fashion. Three trials for each of the three pendulums were collected, and average periods and amplitudes were computed per trial. The mean values for the three trials per pendulum are reported in Table 1 for all 6 participants.

Comparison across participants shows that, indeed, for a given pendulum, different periods and amplitudes were selected. However, when comparing values within a participant, a systematic scaling for the three pendulums was evident in every case. The range of periods performed in the three trials, listed in parentheses, shows the high consistency of periods over repeated trials. Similarly, the amplitudes tended to scale with the period, so that longer periods were associated with larger amplitudes. However, these values were less systematic than the period results. Hence, for the three experimental sessions, a constant amplitude of 0.52 rad was chosen that approximately represented the average amplitude observed in previous experiments. Note, however, that this value was found to be below the overall mean of the present experiment. To obtain the best possible matching of target period manipulations with these preferred periods from the preparatory trials, the data collection for the experiment proper was conducted immediately after these preparatory trials.

For a first impression of the participants' performance, an exemplary trial's time series of angular displacement together with the target signal is shown in Figure 3. This trial was performed with pendulum P1000 for a period asymmetry of  $\delta = 100$  ms; that is, the target period was 100 ms longer than the individually preferred period for this pendulum. For clarity, only the synchro-

Table 1  
Average Preferred Periods (in Milliseconds) and Amplitudes (in Radians) for Each Participant as Calculated From Three Trials Conducted for Each Pendulum in a Preparatory Session

Participant	P800		P1000		P1200	
	Period	Amplitude	Period	Amplitude	Period	Amplitude
1	704 (10)	0.561 (0.059)	775 (17)	0.588 (0.031)	1,075 (22)	0.616 (0.124)
2	654 (18)	0.623 (0.154)	667 (31)	0.577 (0.013)	885 (58)	0.632 (0.251)
3	806 (22)	0.736 (0.211)	885 (10)	0.728 (0.021)	1,124 (75)	0.875 (0.173)
4	575 (15)	0.726 (0.060)	806 (9)	0.745 (0.037)	1,020 (16)	0.807 (0.103)
5	901 (42)	0.642 (0.025)	1,020 (28)	0.801 (0.050)	1,299 (96)	0.853 (0.090)
6	952 (36)	1.103 (0.079)	1,031 (56)	1.064 (0.047)	1,124 (31)	1.064 (0.097)

Note. The values in parentheses show the range calculated between minimum and maximum values for the average periods and amplitudes observed in the three trials. P800, P1000, and P1200 are the three pendulum conditions.

nization segment *S* and the first continuation segment *CI* are displayed. During *S* the participant was clearly able to match the target period and amplitude relatively well and remained close to an inphase coordination with the target signal. However, with beginning *CI* at 20 s, the pendular movements began to deviate from the target signal, which was not seen by the participants but is extrapolated here for better visualization. As to be expected for the condition  $\delta = 100$  ms, within the first 16 s of *CI* the participants sped up their oscillation and inserted one entire cycle compared with the target signal. Also, the midpoint of the amplitude changed in this trial, whereas the overall amplitude changed only little. The goal of the following analyses was to extract regularities as seen in this representative pattern of period deviations and variability.

#### Mean Cycle Analysis: Period and Amplitude

The first focus of analysis was on the peak-to-peak periods *T* corresponding to the intertap intervals in the tapping literature. To assess the accuracy of the participants' performance or, conversely, the deviation from the target period, linear regressions were performed, where for each trial segment the average performed *T* was regressed against the respective target period. As the

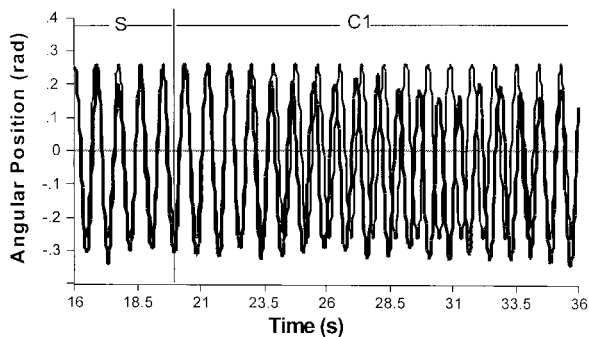


Figure 3. A segment *S* of a time series between 16 s and 36 s showing the target oscillation (thin line) and the pendular movement (thick line). Three cycles after turning off the metronome in *CI*, period and amplitude of the pendular trajectory start to deviate visibly from the initial oscillatory target signal.

absolute values of the preferred and target periods differed across participants, separate regressions had to be conducted for each participant, each pendulum, and each segment, giving a total of 12 regressions per participant. Each regression was performed for 14 data points (i.e., two trials for seven target period conditions). If the target periods were accurately produced, the linear regression slope would be 1, and the intercept 0.

In Table 2 the large number of regressions is summarized by showing mean values of regression slopes and intercepts for each pendulum, averaged across all participants. In accordance with Prediction 1, during *S* the slopes and intercepts of the linear regressions for all three pendulums in all participants were not significantly different from 1 and 0, respectively. All regressions had  $r^2$  values of .99 or 1. Throughout the continuation segments, however, the slopes monotonically decreased within each participant, whereas the regression  $r^2$  values were still .88 and higher. This decrease in slope was associated with a monotonic increase in the intercept. The systematic decrease in slope and the increase in the intercept were evident for all cases. These significant trends in the regressions indicate that there was a systematic change in the periods of *C* toward the preferred periods.

To further quantify this systematic drift, the difference between target periods and actual performed cycle periods  $\Delta T$  were calculated for each of the synchronization and continuation segments. Positive  $\Delta T$  values were obtained when the actual periods were shorter than the target period (accelerating trend); negative values were obtained when participants' actual periods were longer than the target period.

A 3 (pendulum)  $\times$  7 ( $\delta$ )  $\times$  4 (segment) ANOVA was performed with  $\Delta T$  as the dependent measure. There was a significant three-way interaction,  $F(36, 180) = 1.66, p < .05$ . A central result with respect to Prediction 1 was the significant interaction of  $\delta$  and segment,  $F(18, 90) = 10.48, p < .0001$ . Further significant interactions were found for pendulum and  $\delta$ ,  $F(12, 60) = 2.01, p < .05$ , and for pendulum and segment,  $F(6, 30) = 2.75, p < .05$ . Last, the main effect for  $\delta$  was also significant,  $F(6, 30) = 15.71, p < .0001$ . Figure 4 illustrates the central result, showing  $\Delta T$  against  $\delta$ , the difference between the target period minus preferred period. In support of Prediction 1,  $\Delta T$  was positive for target periods longer than the preferred period ( $\delta > 0$ ).  $\Delta T$  was negative for target periods shorter than the preferred period ( $\delta < 0$ ). Further support-

Table 2  
Accuracy of Periods Produced in the Synchronization and Continuation Segments

Segment	P800		P1000		P1200	
	Intercept	Slope	Intercept	Slope	Intercept	Slope
<i>S</i>	0.003	0.997	0.011	0.989	0.003	0.997
<i>C1</i>	0.018	0.948	-0.002	0.994	0.209	0.803
<i>C2</i>	0.098	0.831	0.067	0.902	0.336	0.674
<i>C3</i>	0.148	0.764	0.139	0.814	0.389	0.630
<i>C</i>	0.090	0.845	0.069	0.901	0.311	0.702

Note. Linear regressions were performed for each participant separately for each pendulum and each segment (*S*, *C1*, *C2*, and *C3*). The tabulated values are average slopes and intercepts (in milliseconds) of the linear regressions across participants performed separately for the three pendulum conditions (P800, P1000, and P1200) and four trial segments. *C* refers to the averaged performance in the 60-s continuation interval.

ing Prediction 1, these deviations increased for increasing  $\delta$ . In accordance with Prediction 2, there was a monotonic increase of  $\Delta T$  from *S* to *C3*, which indicated a consistent drift in the mean periods across segments: As expected,  $\Delta T$  was close to zero during *S* and increased from *C1* to *C3*. Not consistent with the two predictions was the fact that the crossing of lines occurred at  $\delta = -50$  ms, instead of at  $\delta = 0$  ms. This result generally indicated that participants tended to shorten their period during *C*.

The interaction between  $\delta$  and pendulum explains this observation (Figure 5): Although P1200 showed the predicted drift toward the preferred period in the most pronounced way, this behavior was not as marked for the two shorter pendulums, P800 and P1000. Instead, both pendulums had the tendency to speed up regardless of  $\delta$ . This discrepancy underlies the results of Figure 4 where the lines cross at  $\delta = -50$  ms. The interaction between pendulum and segment is also a consequence of this discrepant behavior between the three pendulums.

To test changes in the amplitudes, the amplitude deviations  $\Delta A$  were analyzed with the same  $3$  (pendulum)  $\times$   $7$  ( $\delta$ )  $\times$   $4$  (segment) ANOVA. A significant interaction was identified between  $\delta$  and segment,  $F(18, 90) = 2.04, p < .05$ . As Figure 6 displays, this effect is due to the fact that amplitude deviations were consistently close to zero during *S* for all  $\delta$ . In contrast, there was a small but monotonic increase in  $\Delta A$  from *C1* to *C3* that was more pro-

nounced for positive  $\delta$  values. As noted above, the positive  $\Delta A$  values signal that the preferred amplitudes were commonly larger than the target amplitude. Hence, in accordance with the drifts in the period, the amplitude also changed consistently toward the preferred value. In correspondence, for negative  $\delta$  there were smaller period deviations accompanied by smaller amplitude deviations.

#### Variability in Periods and Amplitudes

Turning to Predictions 3 and 4, the variability estimates were regressed against  $\delta$ . As a first statistical estimate for period variability, the standard deviations of cycle periods *SDT*, were calculated separately for each segment. Subsequently, the mean values of *SDT* across all participants for each segment were regressed against  $\delta$  using a second-order polynomial. No significant results were obtained. Instead, for all segments *SDT* increased monotonically with increasing positive  $\delta$ , which corresponds to increasing target period. This observation was statistically supported by the same  $3 \times 7 \times 4$  ANOVA as above, which produced a main effect for  $\delta$ ,  $F(6, 30) = 18.75, p < .001$ . Although this result is not in accordance with Prediction 3, it is a robust effect in the timing literature that variability increases with the mean period duration. In addition, a tendency for a segment main effect was seen, but this did not reach significance when all participants were included. A close inspection of the data revealed that one participant showed

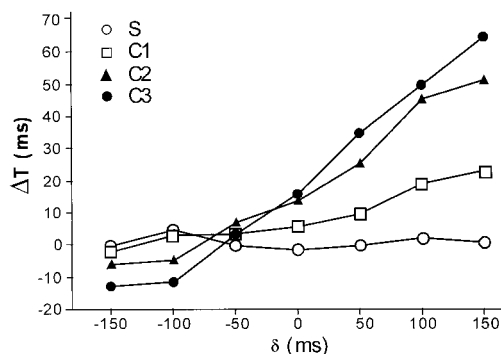


Figure 4. Mean differences between the target period and the actually performed period  $\Delta T$  in the synchronization segment *S* and continuation segments *C1*, *C2*, and *C3* for the seven delta period conditions ( $\delta$ ), averaged across pendulums. The data are averages across all participants.

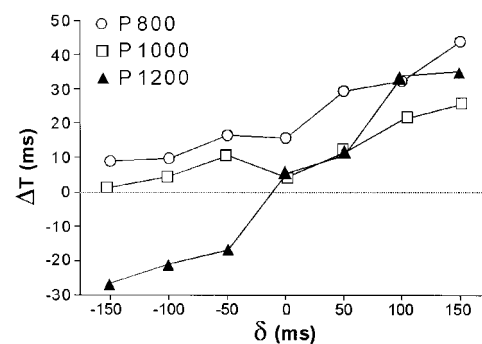


Figure 5. Mean differences between the target period and the actually performed period  $\Delta T$  for the three different pendulums, averaged across segments. The data are averages across all participants.  $\delta =$  delta period.

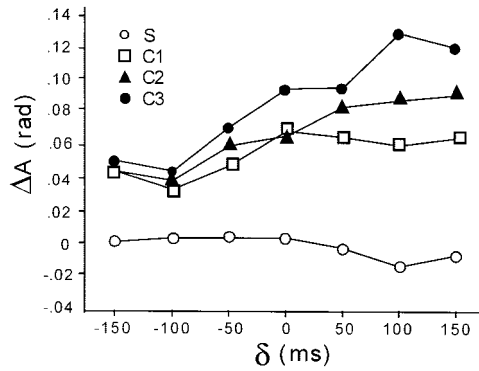


Figure 6. Overall amplitude deviations,  $\Delta A$ , in the synchronization segment  $S$  and continuation segments  $C1$ ,  $C2$ , and  $C3$  for the seven delta period conditions ( $\delta$ ). The data are averages across all participants.

an increased variability, which was possibly due to fatigue. When this participant was eliminated from the analysis, the segment main effect became significant, without affecting any other results,  $F(3, 15) = 6.15, p < .01$ . In support of Prediction 4,  $SDT$  decreased from  $S$  to  $C3$  showing that with the participants' drift toward their preferred periods, movements became less variable.

To further pursue Predictions 3 and 4, the  $SDT$  values were normalized by their mean periods, that is the coefficient of variation (CVT) was calculated. Performing the same polynomial regressions for CVT against  $\delta$ , a significant U-shaped function was observed in segment  $S, r^2 = .81; CVT = .047 - .006\delta + .001\delta^2$ , with a significant second-order coefficient ( $p < .05$ ). The minimum is close to  $\delta = 0$ . For  $C1, C2$ , and  $C3$ , this U shape disappeared and polynomial regressions were no longer significant (Figure 7). In order to detect differences in the pendulums, CVT was submitted to a  $3 \times 7 \times 4$  ANOVA. A main effect for pendulum was detected,  $F(2, 10) = 14.06, p < .001$ , showing that P800 had the highest and P1200 had the lowest CVT.

Analogous to period variability, the variability of the performed amplitudes  $A$  was captured by their standard deviations  $SDA$ . Testing for the U-shaped dependency of variability on  $\delta$ , a polynomial regression was conducted. Figure 8 shows the highly significant result when values were collapsed across all segments

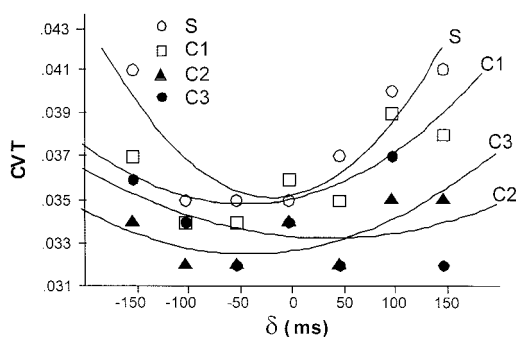


Figure 7. Coefficient of variation of period (CVT) as a function of delta period ( $\delta$ ). The lines represent the second-order polynomial regressions performed on the average values obtained for the different segments  $S, C1, C2$ , and  $C3$ . The data are averages across all participants.

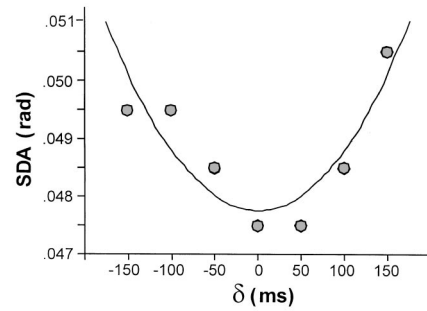


Figure 8. Standard deviations of amplitude ( $SDA$ ) as a function of delta period  $\delta$ . The data are averages across all segments, pendulums, and participants. The line shows a second-order polynomial regression.

( $R^2 = .78; SDA = .052 - .002\delta + .003\delta^2$ ). No U shape was obtained for the individual segments.

Inspection of the data revealed that the variability was highest in  $C1$  and significantly different from  $S, C2$ , and  $C3$  (mean values:  $S, 0.049$  rad;  $C1, 0.058$  rad;  $C2, 0.050$  rad;  $C3, 0.050$  rad). To test for significant differences between the segments and pendulums, an ANOVA was performed. Only the main effect for segment was significant,  $F(3, 15) = 4.18, p < .05$ . This highlights that as soon as the explicit visual target constraints disappeared, the amplitudes changed toward their preferred larger values, leading to a markedly increased variability in this first segment. It can be concluded that the amplitude constraints were more severe during  $S$ , and immediately after switching off the target, participants adapted their amplitude to their preferred value. This was already seen in Figure 4, where a large difference in amplitude occurred between  $S$  and  $C1$ .

### Fluctuations of Continuous Trajectories

Thus far, only the behavior of complete cycles was analyzed. One goal of the study was to also evaluate the continuous trajectories and their change throughout the synchronization and continuation segments for the given target-pendulum pairings. One approach to quantify the shape and variability of the trajectory is to capture the deviations from a harmonic wave by the measure harmonicity,  $H$ , as  $H$  is defined in phase space and it captures fluctuations in the behavior in both state variables position and velocity. To test Predictions 3 and 4 (Figure 1B) second-order polynomial regressions were performed on  $H$  against  $\delta$ , separately for each segment. Figure 9 displays these regressions: In support of Prediction 3,  $H$  was generally lowest for  $\delta = 0$  and it increased with increasing deviations from  $\delta = 0$ . The polynomial regression was significant for  $S$  ( $r^2 = .81$ ), but only marginally for  $C1$  and no longer for  $C2$  and  $C3$ . This result expresses that pendulum-target pairings with differing eigenperiods are less stable and associated with higher levels of fluctuations. Note that this prediction is still visible in  $C1$ , but no longer in  $C2$  and  $C3$ . This result complements the results on amplitude and period variability above, which showed the highest variability in the segment  $C1$  that immediately followed after the metronome was turned off.

In addition, the  $H$  values were submitted to the same ANOVA as above. The interaction between segment and  $\delta$  was significant,  $F(18, 90) = 1.93, p < .05$ . Also, the main effect of pendulum was

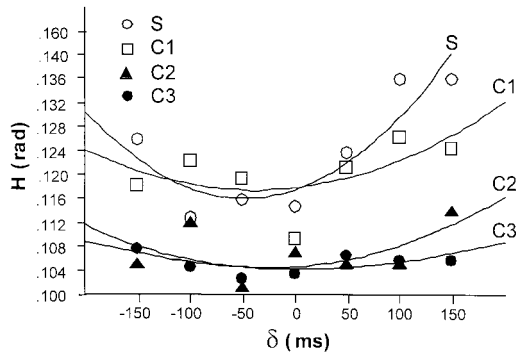


Figure 9. Harmonicity,  $H$ , as a function of delta period  $\delta$ . The lines represent the second-order polynomial regressions performed on the average values obtained for the different segments  $S$ ,  $C1$ ,  $C2$ , and  $C3$ . The data are averages across all pendulums and participants.

significant, with  $F(2, 10) = 21.62, p < .01$ . As expected from the symmetric U shape, the main effect for segment did not reach significance. The pendulum effect expressed a decrease in  $H$  from P800 to P1200. This can be attributed to the filtering effect that pendulum with longer eigenperiod have.

*Autocorrelations and Clock and Motor Variance*

Given the emphasis of the present investigation on the discrepancy between the target period and the preferred period that is mechanically and physiologically determined, a clock-motor analysis was performed on the sequence of cycle periods during the entire continuation segment (Wing & Kristofferson, 1973a). The first step in testing for clock and motor variance is an autocorrelation analysis, in which two predictions from the model were tested: Lag 1 autocorrelation between successive periods should be negative between 0 and  $-0.5$ ; Lag 2 and all other autocorrelations should be zero. Because of the identified significant drifts in  $C$ , positive autocorrelations had to be expected. Hence, linear regressions were performed over the individual continuation segments and the slopes were subtracted from the individual cycle periods. Table 3 summarizes the autocorrelation results of Lag 1 and Lag 2 of all trials of all 6 participants. No higher lags were calculated as there were too few data points to warrant the analysis. In only 23% of all trials were the Lag 1 autocorrelations between  $-0.5$  and 0.

For Lag 2 autocorrelations, 70% were not significantly different from zero. Especially the positive Lag 1 autocorrelation makes the application of the clock-motor decomposition unreasonable as negative clock and motor variances would be obtained. Note that these numbers were obtained after a significant drift was eliminated.

*Time Course of the Drift*

Motivated by the oscillator-based perspective, we hypothesized an exponential approach to the preferred period after the driving oscillator, visual target, had been turned off (Prediction 5). To test this prediction the series of individual cycle errors  $\Delta T$  were fitted with an exponential function  $\Delta T = (a - b)e^{-cx}$  across the entire continuation segment. Figures 10A and 11A illustrate the exponential time course of this drift for two trials: In Figure 10A, a trial with  $\delta = 100$  ms (P1000) exemplifies how the period deviations increased throughout the continuation segment and, thereby, the cycle periods approached the preferred period. The exponential fit was significant with an  $r^2 = .74$ . Similarly, Figure 11A shows a decrease in cycle period throughout the 60 s for a trial with  $\delta = -150$  ms approaching the slower preferred period (P1200). The exponential fit was significant with  $r^2 = .67$ .

For different  $\delta$ , different exponential approaches were expected: the larger  $\delta$ , the steeper the approach toward the preferred period. Figure 12 shows a summary graph with exponential fits for individual trials selected from each  $\delta$  condition all performed with P1200 by one participant. For clarity, the data points were omitted from the graph and only the fitted functions were displayed. All fits were significant ( $p < .05$ ). The thick lines pertain to  $\delta = \pm 150$  ms; the dashed line pertains to  $\delta = 0$ ; and the two intermediate thin lines belong to  $\delta = \pm 50$  and  $\pm 100$  ms. There was an incremental increase in the steepness of the exponential function with increasing asymmetry  $\delta$ .

*Long-Range Correlations Across Cycles*

The results of both the autocorrelation analyses and the exponential fits spoke to longer range correlations beyond the hypothesized stochastic model of Wing and Kristofferson (1973a, 1973b). In order to further highlight such trends, we smoothed the data using a three-point averaging window. Figures 10B and 11B show the same trial as in the first panel where the sequence of  $\Delta T$  was

Table 3  
Autocorrelation Analysis With Lag 1 and Lag 2 Performed on Continuation Segments of Individual Trials for All Participants

Participant	P800					P1000					P1200				
	Lag 1		Lag 2			Lag 1		Lag 2			Lag 1		Lag 2		
	-0.5-0	> 0	= 0	> 0	< 0	-0.5-0	> 0	= 0	> 0	< 0	-0.5-0	> 0	= 0	> 0	< 0
1	2	12	4	10	0	0	14	4	10	0	0	14	5	9	0
2	12	2	12	2	0	1	13	6	8	0	3	11	8	6	0
3	6	8	12	2	0	2	12	12	2	0	3	9	14	0	0
4	2	12	4	10	0	2	12	12	2	0	0	14	6	8	0
5	4	10	14	0	0	2	12	13	1	0	4	10	13	1	0
6	5	9	14	0	0	4	10	13	1	0	6	8	11	3	0

Note. The time series were detrended before the autocorrelation tests were conducted. P800, P1000, and P1200 are the three pendulum conditions.

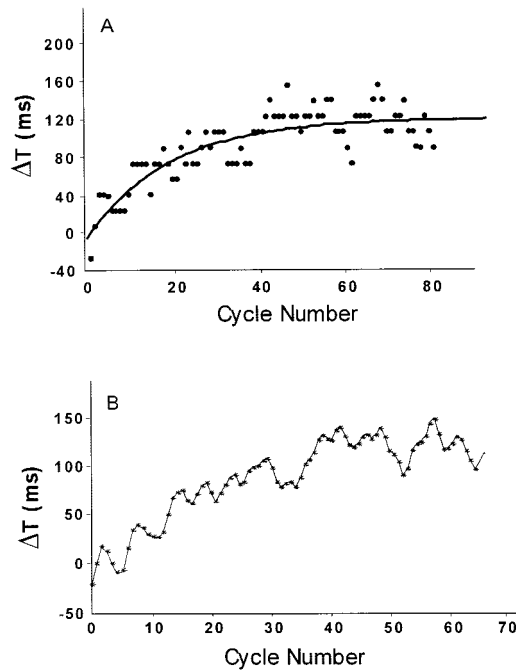


Figure 10. A: Series of cycle errors,  $\Delta T$ , across the continuation segment. The line represents an exponential fit to the data. The condition was  $\delta = 100$  ms performed with the pendulum P1000. B: Series of cycle errors,  $\Delta T$ , across the continuation segment, which were smoothed to highlight fluctuations spanning 3–6 data points.

smoothed. As is evident from these two exemplary trials, cyclic fluctuations can be discerned that span data points.

### Discussion

In order to elucidate the nature of rhythmic movement generation, a host of studies have been performed on periodic tapping movements. The primary focus of analysis has been on the variability of the intertap intervals, argued to provide a window into the nature of the intrinsic timing mechanisms. Most frequently, the so-called continuation paradigm was used. Reasons for this choice was that during the initial synchronization phase participants could be instructed to perform any given period, which were typically set within the range of 100 and 1,000 ms. The tasks involved synchronizing finger flexions to touch a surface with each auditory signal. After having established the periodic process, the metronome was switched off so that the clocking processes were free to unfold during a continuation interval. The absence of metronome beeps was advantageous because otherwise beeps would provide comparative signals and include feedback-based corrective processes that interfered with the intrinsic timing mechanisms. Typically, the continuation phase was confined to 20 to 40 taps, mostly to avoid the interference of any period drifts.

There has been a wealth of theorizing about the nature of these intrinsic timekeeping processes, discussing, for example, the fixed or adaptive nature of an internal clock, linear and quasi-linear models, the hierarchical representation of temporal intervals, or multiple timer models (Ivry & Richardson, 2002; Miall, 1996; Semjen, 2002; Vorberg & Wing, 1996). More recently, informa-

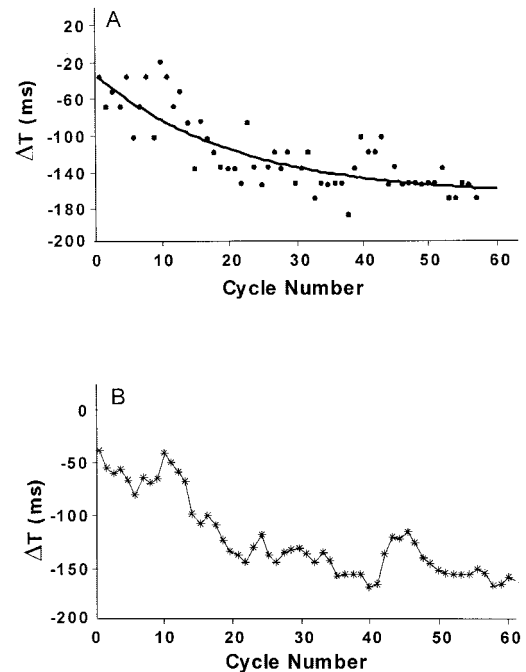


Figure 11. A: Series of cycle errors,  $\Delta T$ , across the continuation segment. The line represents an exponential fit to the data. The condition was  $\delta = -150$  ms performed with the pendulum P1200. B: Series of cycle errors,  $\Delta T$ , across the continuation segment, which were smoothed to highlight fluctuations spanning 3–6 data points.

tion-processing approaches have been challenged or complemented with oscillator-based accounts (Daffertshofer, 1998; Peper, Beek, & Daffertshofer, 2000; Pressing, 1998; Schöner, 2002). Studies on lesions or pathologies, particularly of the cerebellum and the basal ganglia (Parkinson's disease), have highlighted the role of these cerebral structures in timing (e.g., Franz, Ivry, & Helmuth, 1996; Ivry & Keele, 1989; Ivry, Keele, & Diener, 1988; Welsh, Lang, Sugihara, & Llinas, 1995). Imaging studies aimed at elucidating the underlying cortical structures in healthy popula-

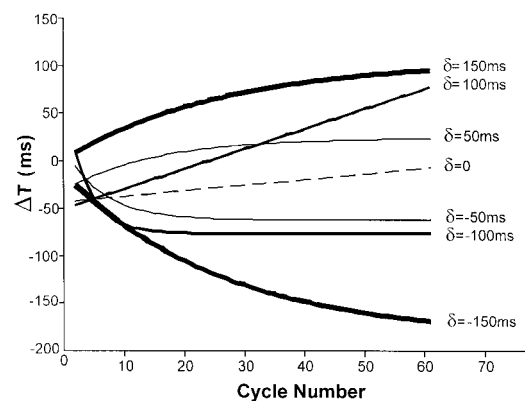


Figure 12. Exponential fits on cycle errors,  $\Delta T$ , against cycle number in the continuation segment. The fits were performed on single trials with seven different delta period ( $\delta$ ) conditions performed by 1 participant with pendulum P1200.

tions have complemented the above research (Macar, Vidal, & Casini, 1999; Rao et al., 1996, 1997; Wing, 2002).

The contribution of peripheral processes arising between the issuing of the motor command and the overt behavior has been discussed. Most notably, the two-process model of timing developed by Wing and Kristofferson has been applied to tapping data under a variety of different experimental manipulations and different populations (Wing & Kristofferson, 1973a, 1973b; for a recent overview, see Wing, 2002). This model assumes that two independent processes underlie the generation of each interval, namely a timekeeper or clock mechanism and a peripheral delay. Independent noise sources are added to both the clock interval and the motor delay. This conceptualization essentially regards the generation as a sequence of discrete events, each associated with Gaussian noise. Conforming to the model's predictions, empirical studies of continuation tapping have found that increasing the target periods leads to greater clock variance, whereas little or no change has been observed for the motor variance.

Given these theoretical arguments, remarkably little empirical and theoretical work has been devoted to explicitly extricating the contribution of the biomechanical and neurophysiological properties of the plant. Although various studies have compared tapping behavior when performed by different effectors, such as finger, wrist, and elbow, the results were equivocal and often led to a rejection of the relevance of these properties. For instance, Wing (1977) compared tapping performed by finger flexion, wrist flexion, forearm pronation and supination, and elevation. Contrary to expectation, he found that it was clock variance, not motor variance, that decreased with limb size. The study also showed that the variance in the movement period was a function of the particular effector. Specifically, finger flexion led to the greatest variability followed by wrist flexion, followed by forearm pronation and supination, with the least variance observed for forearm elevation. However, only a small range of target periods were studied, and it is also not clear from this experiment whether the variability is related to the limb's inertia alone or the asymmetry between the target motion and effector. Collyer et al. (1992) explicitly rejected the influence of biomechanical determinants.

A direct assessment of the role of dynamic properties of the effectors and their effect on the structure of the variance was performed by Turvey and colleagues (Turvey, Rosenblum, & Schmidt, 1986; Turvey, Schmidt, & Rosenblum, 1989). Using bimanual wrist-pendulum movements, similar to the movements of this study, the authors showed that for antiphase oscillations, increasing asymmetry between the effectors led to greater motor variance, whereas clock variance remained unaffected, interpreted as support for a single clocking mechanism for both oscillating hands. On the other hand, comparing inphase and antiphase oscillations, clock variance differed but motor variance was unaffected for comparable pendulum pairings. Different from the typical continuation paradigm, in Turvey et al.'s (1989) studies no target frequency was prescribed. Participants self-selected their movement frequency, which, consequently, was dependent on and covaried with the pairing of pendulums they were given. Aside from this study, the examination on such biomechanical influences have been few and far between and the results have been somewhat equivocal. The bulk of studies and theorizing has focused on internal timing processes and their neural underpinnings.

The present study aimed to directly examine the role of biomechanical and neuromuscular properties of the effectors and the asymmetry between the task and effector in timing and variability of rhythmic movements. In the face of the large number of theoretical propositions, it is worth pointing out that most studies have limited their investigations to finger-tapping movements, and almost exclusively, it has been the time intervals between successive contacts that have been studied. We argue that for a more general theory of timing, a greater variety of movement types must be investigated and the continuous trajectories must be taken into consideration. Within this overall objective, the present study had several goals.

First, instead of finger tapping we used wrist actions extended by handheld pendulums with exchangeable lengths and weights. This setup permitted the easy manipulation of the inertial properties of the limb. In addition, in pendular movements the timing preferences due to intrinsic dynamics are more pronounced as pendular movements are centered around the direction of gravity, facilitating the computation of the mechanical resonance frequency. Additional neuromuscular properties were included in the assessment because it was the individually preferred period and not the mechanically calculated period that provided the landmark for manipulations of the target periods.

Second, we aimed to study the relation between this intrinsically preferred period with the target period, hypothesizing that the accuracy and variability in performance critically depends on this symmetry or asymmetry. Previous work on sinusoidal tracking with different effectors has already given support that it is this relative timing relation that accounts for systematic phase relations and fluctuations in the tracking trajectory. If the effector's period was slower (faster) there was an increasing phase lag (lead) between the target and the effector, and conversely (Russell et al., 2003; Russell & Sternad, 2001). By the explicit quantitative manipulation of the relation between target period and preferred periods of the moving wrist-pendulums, we directly assessed the influence of the task-effector asymmetry on the performance in a continuation paradigm.

Third, as the focus is on the intrinsically driven effects during continuation, each trial included an extended continuation phase. Although the continuation segment has typically been limited to maximally 50 taps to prevent drifts to interfere, we explicitly extended the continuation phase to 60 s to allow these processes to rise to prominence for better analysis. Period drifts have commonly been regarded rather as a nuisance than an effect worthy of study, and no clear theoretical attention has been devoted to the drift (exceptions are the studies by Collyer & Church, 1998, and Madison, 2001). When such drifts were noticed, the effect has often been removed by detrending procedures. We hypothesize that it substantially contributes to the variability observed.

Fourth, we collected kinematic data from the entire trajectories that allowed the assessment of changes not only in discrete intertap intervals but also in continuous kinematic measures. The expectations about the period drifts and the degree of fluctuations were formulated in five predictions that were closely derived from work on coupled oscillators as developed for bimanual coordination (Amazeen, Amazeen, & Turvey, 1998; Sternad et al., 1995, 1996). Specifically, we predicted patterns of drift and variability during steady-state oscillations as a function of the asymmetry between the oscillating limb and the target period as schematically sketched

in Figures 1A and 1B. For a model that generates the five predictions, see the Appendix.

### *Systematic Drift Toward the Preferred Period*

The performed periods across the continuation segments showed a marked drift toward the preferred period that supported Prediction 1. Although this trend was purposely enhanced with the comparatively long continuation segment, it needs to be highlighted that this drift was observed from the first continuation segment onward. Hence, this result emphasizes that this tendency cannot be ignored even when only shorter continuation intervals are studied. Although the pattern is in overall agreement with Prediction 1, the average durations of the drifts showed that the participants did not entirely return to their preferred periods but followed the instruction to maintain the initial target period as best they can. The pattern was also consistent with Prediction 2 in that for greater asymmetry between target period and eigenperiod, the drifts were larger. In addition, an overall tendency for an acceleration was observed. Such a tendency for acceleration in long free-tapping trials has been previously documented in a tapping task with additional force constraints by Sternad et al. (2000). With respect to an explicit quantitative model for this drift behavior, note that the relaxation process in the present task is relatively long, virtually lasting 60 s. This duration reflects a much longer time scale than the one observed for a van der Pol oscillator relaxing to its resonance frequency (see Appendix). Depending on the intrinsic damping, the relaxation process is typically of the order of several cycles at most. In order to model the present behavior quantitatively, frequency may also have to be a state variable, as was for instance done by Large and Jones (1999). Alternatively, the modeling has to be expanded to a multilayered system and address more explicitly the influence of an inertial system (e.g., Beek, Peper, & Daffertshofer, 2002; Sternad, Saltzman, & Turvey, 1998).

This drift in the mean cycle values was evident in both periods and amplitudes. Given that continuous data were collected, the amplitude measure is unique for this experimental task and the visual synchronization signal specified both period and amplitude. Note that, counter to expectations, the movement amplitudes increased for all  $\delta$  conditions and, also, when the cycle periods shortened. This effect runs counter to other results on spatiotemporal features of oscillatory movements where shortening of periods is accompanied by a concomitant shortening of amplitudes (Kay, Kelso, Saltzman, & Schönner, 1987). This shows that unconstrained movements clearly tended to larger amplitudes and, in conjunction with faster periods, to higher movement velocities.

### *Variability Throughout the Continuation Phase*

Given these changes in the average spatiotemporal parameters from the first continuation segment onward, changes in variability can be expected. However, the slow changes in period would lead only to the expectation of an increase in variability from the synchronization phase to the continuation phases. The pattern predicted by Prediction 4 is contrary: The variability should decrease throughout the continuation phase because the system moves closer to resonance. This regime is more stable and, hence, accompanied by less fluctuations. The results in Figures 7 and 9

give support to this prediction. Given that participants performed closer to their own preferred spatiotemporal organization, fluctuations decreased. This result also manifests that the presence of the target provides an external forcing that, when switched off, allows the oscillation to adopt a self-driven organization that was presumably closer to resonance. This result is in accord with a study that showed that pendular movements performed at resonance require less control or have fewer active degrees of freedom (Goodman et al., 2000).

Prediction 3 stated that variability is at a minimum when there is symmetry between the target period and the eigenperiod. With increasing asymmetry, variability increases in a U-shaped fashion. This prediction was reported several times for bimannually coupled oscillations (Schmidt et al., 1993; Sternad et al., 1996) and for oscillations with a visual target with and without feedback (Russell et al., 2003; Russell & Sternad, 2001). Indeed, this pattern was again observed in the continuation paradigm. Note that in other respects, the data conform with robust results in the literature. The unnormalized measure of variability, the standard deviations of the cycle periods, showed the monotonic increase with the duration of the movement period. This result reflects the scaling of resolution in timing replicating the expectations from Weber's law.

### *Continuous Nature of the Oscillatory Regime*

The pattern of variability was also obtained when the continuous trajectories were analyzed. The wave-like trajectories were compared with a pure harmonic wave, which is a close approximation to merely mechanical pendular movements at moderate angular excursions. This continuous measure of  $H$  emphasized that not only discrete intervals reflect discrepancies from resonance—assuming that the preferred period corresponds to oscillations at resonance—but that also the entire trajectory of each cycle is affected by the different levels of stability.

The continuous nature of the regime was highlighted in one other way when Wing–Kristofferson's decomposition into clock and motor variance was performed (Wing & Kristofferson, 1973a, 1973b). The present data showed resilient positive Lag 1 autocorrelation, counter to the predicted negative autocorrelations. This effect remained positive even after the trend in periods was removed with a linear detrending operation. Autocorrelations were still positive and significant with lags up to 3–6 data points. This result, revealing long-term correlations across several cycles, is in contradiction to the essential assumption in the Wing–Kristofferson model that each temporal interval is essentially a discrete independent event. From an oscillator perspective, rhythmic movements are not a sequence of concatenated cycles, or intertap intervals, but rather a regime that is parameterized in terms of some generalized linear and nonlinear stiffness and viscosity parameters. Once set, and with the energy loss and input at a steady state, the movement unfolds in a continuous fashion and longer term correlations are inherent. These long-term correlations are seen when the individual periods are plotted over time. Especially when a smoothing algorithm is applied, cyclic variations over 10 cycles can be discerned.

Although this is left as a topic for further study, one last observation consistent with the interpretation of a dynamic regime should conclude this study: The return to the preferred period throughout the continuation segment showed an exponential shape.

The type of exponential approach is different for the different asymmetry conditions, reflected in different coefficients of the exponential function. Such exponential changes in behavior have been argued as a signature for an underlying dynamical system (Newell, Liu, & Meyer-Kress, 2001).

### Conclusion

Although all these results show marked differences as well as similarities with previous results of studies on finger tapping, it should be pointed out again that the experimental task differed in many respects from the traditional tapping task. First, we used visual stimuli that were presented in a continuous fashion during the synchronization phase. This presentation of timing intervals may have been less marked, and participants may be more prone to forget the target period. Second, we used a pendular movement in which the dynamic component was prominent and the task had no contact events (i.e., taps). In previous work we even argued that the tapping contact itself is a critical event that introduces perturbations to the movement trajectory (Sternad et al., 2000). In fact, explicit target forces had a systematic influence on the observed timing and force variability. Thus, although the continuous nature of the movements possibly enhanced the effects that we aimed to highlight, this feature is by no means absent in other periodic movement forms and warrants investigation. To conclude, these differences in task were intentional in order to highlight neglected aspects of studies on rhythmic timing, and it cannot be excluded that many results may be germane to these modifications in task. And yet, any theory of timing should encompass features that are inherent in all rhythmic tasks and not only tapping tasks.

### References

- Amazeen, P. G., Amazeen, E. L., & Turvey, M. T. (1998). Dynamics of human intersegmental coordination: Theory and research. In D. A. Rosenbaum & C. E. Collyer (Eds.), *Timing of behavior: Neural, computational, and psychological perspectives* (pp. 237–259). Cambridge, MA: MIT Press.
- Bartlett, N. R., & Bartlett, S. C. (1959). Synchronization of a motor response with an anticipated sensory event. *Psychological Review*, *66*, 203–218.
- Beek, P. J., Peper, C. E., Daffertshofer, A. (2002). Modeling rhythmic interlimb coordination: Beyond the Haken-Kelso-Bunz model. *Brain and Cognition*, *48*, 149–165.
- Bernstein, N. (1967). *The coordination and regulation of movement*. London: Pergamon Press.
- Challis, J. H. (1999). A procedure for the automatic determination of filter cut-off frequency for the processing of biomechanical data. *Journal of Applied Biomechanics*, *15*, 303–317.
- Church, R. M., & Broadbent, H. A. (1991). A connectionist model of timing. In M. L. Commons, S. Grossberg, & J. E. R. Staddon (Eds.), *Quantitative models of behavior: Neural networks and conditioning* (pp. 225–240). Hillsdale, NJ: Erlbaum.
- Collins, D. R., Sternad, D., & Turvey, M. T. (1996). An experimental note on defining frequency competition in intersegmental coordination dynamics. *Journal of Motor Behavior*, *28*, 299–304.
- Collyer, C. E., Boatright-Horowitz, S. S., & Hooper, S. (1997). A motor timing experiment implemented using a musical instrument digital interface (MIDI) approach. *Behavior Research Methods, Instruments, & Computers*, *29*, 346–352.
- Collyer, C. E., Broadbent, H. A., & Church, R. M. (1992). Categorical time production: Evidence for discrete timing in motor control. *Perception & Psychophysics*, *51*, 134–144.
- Collyer, C. E., Broadbent, H. A., & Church, R. M. (1994). Preferred rates of repetitive timing and categorical time production. *Perception & Psychophysics*, *55*, 443–453.
- Collyer, C. E., & Church, R. M. (1998). Interresponse intervals in continuation tapping. In D. A. Rosenbaum & C. E. Collyer (Eds.), *Timing of behavior: Neural, psychological, and computational* (pp. 63–87). Cambridge, MA: MIT Press.
- Daffertshofer, A. (1998). Effects of noise on the phase dynamics of non-linear oscillators. *Physical Review E*, *58*, 327–338.
- Dempster, W. T. (1955). *Space requirements of the seated operator* (WAD Tech. Rep. No. 55–159). Dayton, OH: Wright-Patterson Air Force Base.
- Franz, E. A., Ivry, R. B., & Helmuth, L. L. (1996). Reduced timing variability in patients with unilateral lesions during bimanual movements. *Journal of Cognitive Neuroscience*, *10*, 107–118.
- Goodman, L., Riley, M. A., Mitra, S., & Turvey, M. T. (2000). Advantages of rhythmic movements at resonance: Minimal active degrees of freedom, minimal noise, and maximal predictability. *Journal of Motor Behavior*, *32*, 3–9.
- Haken, H., Kelso, J. A. S., & Bunz, H. (1985). A theoretical model of phase transition in human hand movements. *Biological Cybernetics*, *51*, 347–356.
- Hatsopoulos, N. G. (1996). Coupling the neural and physical dynamics in rhythmic movements. *Neural Computation*, *8*, 567–581.
- Hatsopoulos, N. G., & Warren, W. H. (1996). Resonance tuning in rhythmic arm movements. *Journal of Motor Behavior*, *28*, 3–14.
- Holt, K. G., Jeng, S. F., Ratcliffe, S. F., & Hamill, J. (1995). Energy cost and stability in preferred human walking. *Journal of Motor Behavior*, *27*, 164–178.
- Hoyt, D. F., & Taylor, C. R. (1981). Gait and the energetics of locomotion in horses. *Nature*, *292*, 239–240.
- Ivry, R. B., & Hazeltine, R. E. (1995). Perception and production of temporal intervals across a range of durations: Evidence for a common timing mechanism. *Journal of Experimental Psychology: Human Perception and Performance*, *21*, 3–18.
- Ivry, R. B., & Keele, S. (1989). Timing functions of the cerebellum. *Journal of Cognitive Neuroscience*, *1*, 136–152.
- Ivry, R. B., Keele, S., & Diener, H. C. (1988). Dissociation of the lateral and medial cerebellum in movement timing and movement execution. *Experimental Brain Research*, *73*, 167–180.
- Ivry, R. B., & Richardson, T. C. (2002). Temporal control and coordination: The multiple timer model. *Brain and Cognition*, *48*, 117–132.
- Kay, B. A., Kelso, J. A. S., Saltzman, E. L., & Schöner, G. (1987). Space-time behavior of single and bimanual rhythmic movements: Data and limit cycle model. *Journal of Experimental Psychology: Human Perception and Performance*, *13*, 178–192.
- Kugler, P. N., & Turvey, M. T. (1987). *Information, natural law, and the self-assembly of rhythmic movement*. Hillsdale, NJ: Erlbaum.
- Large, E. W., & Jones, M. R. (1999). The dynamics of attending. *Psychological Review*, *106*, 119–159.
- Macar, F., Vidal, F., & Casini, L. (1999). The supplementary motor area in motor and sensory timing: Evidence from slow brain potential changes. *Experimental Brain Research*, *125*, 271–280.
- Madison, G. (2001). Variability in isochronous tapping: Higher order dependencies as a function of intertap interval. *Journal of Experimental Psychology: Human Perception and Performance*, *27*, 411–422.
- Miall, C. (1996). Models of neural timing. In M. A. Pastor & J. Artieda (Eds.), *Time, internal clocks and movement* (pp. 69–94). Amsterdam: Elsevier.
- Newell, K. M., Liu, Y.-T., & Meyer-Kress, G. (2001). Time scales in motor learning and development. *Psychological Review*, *108*, 57–82.
- Noble, M., Fitts, P. M., & Warren, C. E. (1955). The frequency response

- of skilled subjects in a pursuit tracking task. *Journal of Experimental Psychology*, *49*, 249–256.
- Peper, C. E., Beek, P. J., & Daffertshofer, A. (2000). Considerations regarding a comprehensive model of (poly)rhythmic movements. In P. Desain & L. Windsor (Eds.), *Rhythm perception and production* (pp. 31–50). Lisse, the Netherlands: Swets & Zeitlinger.
- Pew, R. W., Duffendack, J. C., & Fensch, L. K. (1967). Sine-wave tracking revisited. *IEEE Transactions on Human Factors in Electronics*, *8*, 130–134.
- Poulton, E. C. (1974). *Tracking skill and manual control*. New York: Academic Press.
- Pressing, J. (1998). Referential behavior theory: A framework for multiple perspectives in motor control. In J. P. Piek (Ed.), *Motor behavior and human skill: A multidisciplinary approach* (pp. 357–384). Champaign, IL: Human Kinetics.
- Rao, S. M., Bandettini, P. A., Binder, J. R., Bobholz, J. A., Hammeke, T. A., Stein, E. A., & Hyde, J. S. (1996). Relationship between finger movement rate and functional magnetic resonance signal change in the human primary motor cortex. *Journal of Cerebral Blood Flow Metabolism*, *16*, 1250–1254.
- Rao, S. M., Harrington, D. L., Haaland, K. Y., Bobholz, J. A., Cox, R. W., & Binder, J. R. (1997). Distributed neural systems underlying the timing of movement. *Journal of Neuroscience*, *17*, 5528–5535.
- Russell, D. M., de Rugy, A., & Sternad, D. (2003). *Task–effector asymmetries in a visuomotor task with and without feedback*. Manuscript submitted for publication.
- Russell, D. M., & Sternad, D. (2001). Sinusoidal tracking: Intermittent control or coupled oscillations? *Journal of Motor Behavior*, *33*, 329–349.
- Schmidt, R. C., Shaw, B. K., Turvey, M. T. (1993). Coupling dynamics in interlimb coordination. *Journal of Experimental Psychology: Human Perception and Performance*, *19*, 397–415.
- Schöner, G. (2002). Timing, clocks, and dynamical systems. *Brain and Cognition*, *48*, 31–51.
- Semjen, A. (2002). On the timing basis of bimanual coordination in discrete and continuous tasks. *Brain and Cognition*, *48*, 133–148.
- Sparrow, W. A., & Newell, K. M. (1994). Energy expenditure and motor performance relationships in humans learning a motor task. *Psychophysiology*, *31*, 338–346.
- Sternad, D., Amazeen, E. L., & Turvey, M. T. (1996). Diffusive, synaptic, and synergetic coupling: An evaluation through inphase and antiphase rhythmic movements. *Journal of Motor Behavior*, *28*, 255–269.
- Sternad, D., Collins, D., & Turvey, M. T. (1995). The detuning factor in the dynamics of interlimb rhythmic coordination. *Biological Cybernetics*, *73*, 27–35.
- Sternad, D., Dean, W. J., & Newell, K. M. (2000). Force and timing variability in rhythmic unimanual tapping. *Journal of Motor Behavior*, *32*, 249–268.
- Sternad, D., Saltzman, E. L., & Turvey, M. T. (1998). Interlimb coupling in a simple serial behavior: A task dynamic approach. *Human Movement Science*, *17*, 393–433.
- Sternad, D., Turvey, M. T., & Saltzman, E. L. (1999). Dynamics of 1:2 coordination in rhythmic interlimb movement: I. Generalizing relative phase. *Journal of Motor Behavior*, *31*, 207–223.
- Sternad, D., Turvey, M. T., & Schmidt, R. C. (1992). Average phase difference theory and 1:1 phase entrainment in interlimb coordination. *Biological Cybernetics*, *67*, 223–231.
- Stevens, L. T. (1886). On the time sense. *Mind*, *11*, 393–404.
- Turvey, M. T., & Carello, C. (1995). Dynamics of Bernstein's level of synergies. In M. Latash & M. T. Turvey (Eds.), *On dexterity and its development* (pp. 339–376). Hillsdale, NJ: Erlbaum.
- Turvey, M. T., Rosenblum, L. D., & Schmidt, R. C. (1986). Fluctuations and phase symmetry in coordinated rhythmic movements. *Journal of Experimental Psychology: Human Perception and Performance*, *12*, 564–583.
- Turvey, M. T., Schmidt, R. C., & Rosenblum, L. D. (1989). "Clock" and "motor" components in absolute coordination of rhythmic movements. *Neuroscience*, *33*, 1–10.
- Turvey, M. T., Schmidt, R. C., Rosenblum, D., & Kugler, P. N. (1988). On the time allometry of co-ordinated rhythmic movements. *Theoretical Biology*, *130*, 285–325.
- von Holst, E. (1973). *The behavioral physiology of animal and man: The collected papers of Erich von Holst* (Vol. 1; R. Martin, Ed. & Trans.). Coral Gables, FL: University of Miami Press. (Original work published 1939)
- Vorberg, D., & Wing, A. M. (1996). Modeling variability and dependence in timing. In H. Heuer & S. Keele (Eds.), *Handbook of perception and action* (Vol. 2, pp. 181–262). New York: Academic Press.
- Wang, M. C., & Uhlenbeck, G. E. (1945). On the theory on Brownian motion II. *Reviews of Modern Physics*, *17*, 323–342.
- Welsh, J. P., Lang, E. J., Sugihara, I., & Llinas, R. (1995). Dynamic organization of motor control within the olivocerebellar system. *Nature*, *374*, 453–457.
- Wing, A. M. (1977). Effects of type of movement on the temporal precision of response sequences. *British Journal of Mathematical and Statistical Psychology*, *30*, 60–72.
- Wing, A. M. (2002). Voluntary timing and brain function: An information processing approach. *Brain and Cognition*, *48*, 7–30.
- Wing, A. M., & Kristofferson, A. B., (1973a). The timing of interresponse intervals. *Perception & Psychophysics*, *13*, 455–460.
- Wing, A. M., & Kristofferson, A. B. (1973b). Response delays and the timing of discrete motor responses. *Perception & Psychophysics*, *14*, 5–12.

(Appendix follows)

## Appendix

## A Model to Simulate the Five Predictions

The five predictions are based on fundamental properties of a forced nonlinear oscillator. Specifically, Predictions 1, 2, and 5 can be produced by a weakly nonlinear van der Pol oscillator that is driven by a sinusoidal force. Under a given parameterization, the oscillator displays a limit cycle behavior with a given resonance frequency or period. When the same oscillator is driven by a sinusoidal force, the oscillator's frequency and amplitude are entrained to the driving sinusoid. Once this driving force is turned off, the oscillator resumes its resonance period. The return or relaxation process to the resonance period follows an exponential time course, where initially large changes diminish the closer the period approaches its resonance period.

The predictions for variability (Predictions 3 and 4) can be similarly produced by a van der Pol oscillator with added noise. When driven at resonance, the noise has less effect on the trajectory. When driven away from its resonance period, the noise has a higher perturbing effect on the system. Note that this behavior is not as generic as the period drift and the system can potentially show more complex behavior dependent on the parameterization of the oscillator and its coupling. However, the present predictions were also motivated by stability analyses performed on a coupled oscillator model developed by Haken, Kelso, and Bunz (1985). At the level of state variables, the model consists of two oscillators that are bidirectionally coupled with symmetrical coupling terms. Each of the oscillators is a hybrid of van der Pol and Raleigh oscillators. When the eigenfrequencies of the two oscillators are different, that is, asymmetrical,

stability analyses of the system at steady state show the U-shaped dependency of stability on the asymmetry between two coupled oscillations. Although this analysis holds for bidirectionally coupled oscillators, the pattern of fluctuations, operationalizing stability, has conformed to this prediction in previous work. Hence, these predictions were also robust for experimental tasks that are unidirectionally coupled to external pacemakers, as for instance found in the manual tracking of a visual target (Russell et al., 2003; Russell & Sternad, 2001).

The new aspect of the continuation paradigm is that the paradigm constitutes the case where the oscillatory system is investigated during its relaxation process from a coupled to the uncoupled equilibrium regime. Hence, the predictions for variability capture the properties of a probability distribution of a noisy oscillatory system during its return to equilibrium.

The five predictions as graphically captured in Figures 1 and 2 can also be produced by an effective model that is formulated for the period produced by an oscillatory system with noise:

$$\dot{T} = -\alpha(T - T_0) + \sqrt{Q}\xi_t.$$

$T$  refers to the actual period,  $T_0$  is the eigen- or preferred period,  $\alpha$  is the gain, and  $\sqrt{Q}\xi_t$  is Gaussian white noise (Wang & Uhlenbeck, 1945).

Received April 4, 2002

Revision received August 30, 2002

Accepted November 2, 2002 ■